Iranian Journal of Oil & Gas Science and Technology, Vol. 8 (2019), No. 1, pp. 78-102
http://ijogst.put.ac.ir

CFD Simulation of Parameters Affecting Hydrodynamics of Packed Beds: Effects of Particle Shape, Bed Size, and Bed Length

Saeid Mohammadmahdi[1] and Ali Reza Miroliaei[2*]

[1] M.S. Student, Department of Chemical Engineering, University of Mohaghegh Ardabili, Ardabil, Iran
[2] Assistant Professor, Department of Chemical Engineering, University of Mohaghegh Ardabili, Ardabil, Iran

Received: November 03, 2017; *revised*: December 10, 2017; *accepted*: January 08, 2018

Abstract

Packed bed reactors have many applications in different industries such as chemical, petrochemical, and refinery industries. In this work, the effects of some parameters such as the shape and size of particles, bed size, and bed length on the hydrodynamics of the packed beds containing three spherical, cylindrical, and cubic particles types are investigated using CFD. The effect of the combination of three particles types in a packed bed was also simulated. The simulation results show that flow channeling occurs in some parts of the bed which are not suitably covered by particles. It was also seen that flow channeling in the packed bed with cubic particles are more than those containing spherical and cylindrical particles. According to the CFD simulations, wake and vortex flows are created in all the beds, and the shape of particles affects these phenomena. The comparison of the pressure drop created in the packed beds indicates that the pressure drop in the packed beds having three particle types is lower than the packed beds containing only spherical, cylindrical, or cubic particles. Finally, the numerical results were compared with empirical correlations in the literature and showed good agreement.

Keywords: Bed Size, Flow Pattern, Combination of Particles, Packing Shape, Stationary Points

1. Introduction

Packed bed reactors are an important part of the chemical industries. They have been widely used for the production of chemical materials on commercial scale. For example, these reactors have been used for the synthesis of materials and combustion processes (Rase, 1990), for removing nitrogen oxides from gaseous fuels (Andrigo et al., 1999), and in Fischer-Tropsch synthesis for the production of liquid fuels (Moazami et al., 2015). Due to the interaction between materials in the packed bed reactors, more accurate understanding of the hydrodynamics and its related issues are of special importance. The solid phase, i.e. the catalyst, has different shapes such as spherical, cylindrical, cubic, ring etc. (Ancheyta et al., 2005).

The main problem in packed bed reactors is a high-pressure drop, so the pressure drop in the packed beds has been studied experimentally and numerically. The pressure drop and drag coefficient in square channels were studied by Calis et al. (2001); their results showed good agreement with the

* Corresponding Author:
Email: armiroliaei@uma.ac.ir

LDA measurements. Atmakidis and Kenig (2009) investigated the wall effect on pressure drop in the packed beds, and they compared the CFD results with the empirical correlations of Zhavoronkov et al. (1949) and Reichelt (1972). The hydrodynamics of packed beds with different N was also simulated by Reddy and Joshi (2010). The obtained CFD results showed good agreement with Ergun's equation. The shape effects on the packing density of frustums were studied by Zhao et al. (2011). Their studies showed that the optimal aspect ratio of truncated cones is 0.8 and increases with increasing the radii ratio. Furthermore, they proposed the correlation between the packing density and shape parameters. Allen et al. (2013) investigated the dependence of pressure drop on particle shape, size distribution, packing arrangement, and roughness. They showed that the pressure drop of packed beds changes significantly with randomly packed smooth particles. The effect of operating conditions such as temperature, pressure, and WHSV on the reactor performance in dimethyl ether synthesis from methanol was investigated by Golshadi et al. (2013). Their results showed that the optimum conditions for accessing a conversion of 85% are WHSV=10 $hr.^{-1}$ and T=563.15 K. In addition, they explained that methanol conversion is dependent on the inlet temperature. Vollmari et al. (2015) studied the pressure drop in a packed bed with arbitrary packing shapes both experimentally and numerically. They stated that simulations are in good agreement with experiments depending on the shape and size of particles. The effect of reaction parameters on the performance of Pt/mordenite zeolites for the isomerization of pure n-pentane and the isomerization of pentane isomer mixture was studied by Bayati et al. (2016). They stated that the maximum yield of isopentane is obtained at a temperature of 220 °C. Moreover, they observed that the effects of WHSV and H_2/HC on the catalytic performance in the binary mixtures are similar to those in pure n-pentane isomerization, while the conversion of n-pentane in the two cases is different. Du et al. (2016) studied the effect of the bed voids between the particles on the hydrodynamics of packed beds. They stated that the particle size does not affect the relative void size, but the particle shape significantly affects the void size distribution. They also mentioned a correlation for the void size distribution. Pressure drop in slender packed beds was investigated by Guo et al. (2017), and they found out that the pressure drop in the packed beds depends on the bed structure since a minor change in the bed structure creates a notable pressure drop even in beds having the same porosity. Ghaemi et al. (2017) carried out CO_2 capture using an aqueous solution of NH_3, H_2O, and NaOH and studied the effect of sodium hydroxide concentration on carbon dioxide absorption. They discovered that the absorption rate of carbon dioxide depends on the concentrations of ionic and molecular species in the liquid phase. Also, they observed that the absorption rate of carbon dioxide rises by increasing ammonia and sodium hydroxide.

According to literature surveyed, it is seen that the hydrodynamics of packed beds has been studied with similar particles in the bed, i.e. spherical, cylindrical particles etc., whereas the combination of particles in a packed bed has not been studied. Therefore, in this study, the effects of bed size, the size of particles, and the shape of particles on the hydrodynamics and characteristics of fluid flow are investigated using CFD firstly for similar particles and then for a combination of three particles of spherical, cylindrical, and cubic shapes in a packed bed having a low bed-to-particle-diameter ratio.

2. Empirical correlations for the prediction of packed bed pressure drop

The most usual relation used to predict pressure drop in the packed beds is the empirical equation of Ergun (1952) as it is applicable to a wide range of flow regimes. Ergun's equation estimates pressure drop in the packed beds according to factors such as fluid flow rate, fluid properties (viscosity and density), and packing arrangement (voids) as follows:

$$\frac{\Delta P}{L}=\frac{150\mu(1-\varepsilon)^2}{\varepsilon^3 d_p^2\varphi^2}u_s+\frac{1.75(1-\varepsilon)\rho}{\varepsilon^3 d_p\varphi}u_s^2 \quad (1)$$

where, μ and ρ are the dynamic viscosity and density of fluid, and u_s represents the superficial velocity of fluid; d_p stands for the particle diameter, and ε and φ are porosity and sphericity respectively.

Ergun's equation is reliable for the prediction of pressure drop in the packed beds with the high *N* ratio, but it cannot be applicable to packed bed with a low *N* ratio (N < 10) (Foumeny et al., 1993). Therefore, some researchers used wall effects in Ergun's equation, and some of their correlations are listed in Table 1.

Table 1

Empirical equations for calculating pressure drop in packed beds.

Reference	Equation	Equation Number
Mehta and Hawley (1969)	$\frac{\Delta P}{L}=150\frac{\mu(1-\varepsilon)^2}{\varepsilon^3 d_{pe}^2\varphi^2}u_s M^2+1.75\frac{(1-\varepsilon)\rho}{\varepsilon^3 d_{pe}\varphi}u_s^2 M$	(2)
	$M=1+\frac{4d_{pe}}{6D(1-\varepsilon)}$	(3)
Reichelt (1972)	$\emptyset=\frac{KA_w^2(1-\varepsilon)^2}{Re_{dp}\varepsilon^3\varphi^2}+\frac{A_w(1-\varepsilon)}{B_w\varepsilon^3\varphi}$	(4)
	$A_w=1+\frac{2}{3(D/d_p)(1-\varepsilon)}, B_w=\left[K_1(\frac{d_p}{D})^2+K_2\right]^2, \emptyset=\frac{\Delta P d_{pe}}{L\rho U^2}$	(5)
Montillet et al. (2007)	$\frac{\Delta P}{L}=\alpha\left(\frac{\rho u_s^2}{d_{pe}}\right)\left(\frac{(1-\varepsilon)}{\varepsilon^3}\right)(N)^{0.2}\left(1000{Re_p}^{-1}+60{Re_p}^{-0.5}+12\right)$	(6)

Equations of Table 1 are used for spherical particles, so some researchers determined coefficients in order to utilize these equations for non-spherical particles.

Eisfeld and Schnitzlein (2001) modified the coefficients of Reichelt's equation for a range of beds to particle diameter ratios of $1.624 < N < 250$ by fitting it for spherical and non-spherical particles:

$$\frac{\Delta P}{L}=K\frac{\mu_f(1-\varepsilon)^2}{\varepsilon^3 d_p^2}u_s M^2+\frac{(1-\varepsilon)\rho_f}{\varepsilon^3 d_p}u_s^2\frac{M}{B_w} \quad (7)$$

In the above equations, the coefficients *K*, k_1, and k_2 for spherical particles are 154, 1.15, and 0.87 respectively, and they are respectively 190, 2, and 0.77 for cylindrical particles; for all particles *K*, k_1, and k_2 are 155, 1.2, and 0.83 respectively; d_{sv} should be used instead of d_p for non-spherical particles.

Nemec and Levec (2005) stated Ergun's equation for cylindrical particles as follows:

$$\frac{\Delta P}{L}=\frac{150\mu(1-\varepsilon)^2}{\varepsilon^3 d_{sv}^2\varphi^{3/2}}u_s+\frac{1.75(1-\varepsilon)\rho}{\varepsilon^3 d_{sv}\varphi^{4/3}}u_s^2 \quad (8)$$

Allen et al. (2013) expressed a correlation for the smooth and rough spherical and non-spherical particles:

$$\frac{\Delta P}{L} = \left[\frac{a}{Re_{Duct}} + \frac{b}{Re_{Duct}{}^{c}}\right].\frac{(1-\varepsilon)}{\varepsilon^3}.\frac{\rho_f.u_s^2}{8}.\frac{\sum A_p}{\sum V_p} \quad (9)$$

$$Re_{Duct} = \frac{4\,.\,\rho_f\,.\,u_s}{\mu_f\,.(1-\varepsilon)}.\frac{\sum V_p}{\sum A_p} \quad (10)$$

In Equations 9 and 10, total particle volume to surface ratio is used instead of equivalent diameter. The coefficients *a*, *b*, and *c* for smooth spherical particles are 172, 4.36, and 0.12 respectively, and they are respectively 185, 6.35, and 0.12 for rough spherical particles; *a*, *b*, and *c* are respectively 216, 8.8, and 0.12 for cylindrical particles and 240, 10.8 and 0.1 for cubic particles.

3. CFD modeling

3.1. Governing equations

Momentum and continuity equations are used in order to investigate fluid flow. The continuity equation is defined as follows:

$$\frac{\partial \rho}{\partial t} + \nabla \cdot (\rho u) = 0 \quad (11)$$

The equation for the conservation of momentum is given by:

$$\frac{\partial (\rho u)}{\partial t} + \nabla \cdot (\rho u u) = -\nabla p + \nabla \cdot (\rho \vartheta \nabla u) + \rho g_i \quad (12)$$

where, p is the static pressure, and ρ represents the fluid density; ϑ denotes the kinematic viscosity, and ρg_i is the gravitational force. Two equations must be solved to obtain accurate flow field under different boundary conditions (ANSYS Inc., 2009).

The assumptions and related boundary conditions for the simulations are as follows:

1- Steady-state fluid flow;

2- Incompressible fluid;

3- Constant velocity in the bed inlet;

4- Constant pressure in the bed outlet;

5- SIMPLE algorithm was used for coupling velocity and pressure;

6- Second order upwind discretization method was employed to increase the accuracy of the results;

7- No-slip velocity condition was assumed at the walls and the surface of particles.

The convergence criterion was maintained to achieve the answer with a very low level of residual of about 10^{-6} in equations.

3.2. Characteristics of particles and beds

Packed beds were designed in three different bed to particle diameter ratios of $N = 4.17$, $N = 6.26$, and $N = 9.39$. Three particle shapes of spherical, cylindrical, and cubic were used in the simulations. The characteristics of the particles and the beds are explained in Table 2.

Table 2

Characteristics of the particles and beds.

Particle shape	Dimension [mm]	Porosity [−]	$N = \frac{D}{d_p}$
Spherical	d_p 23 15. 33 10.22	0.55 0.57 0.54	4.17 6.26 9.39
Cylindrical	L_p d_p 23 23 15.33 15.33 10.22 10.22	0.607 0.568 0.576	4.17 6.26 9.39
Cubic	H_p W_p L_p 23 23 23 15.33 15.33 15.33 10.22 10.22 10.22	0.625 0.572 0.586	4.17 6.26 9.39

The air was chosen as the fluid in the packed beds. Figure 1 shows the sample of the designed beds with the different particles.

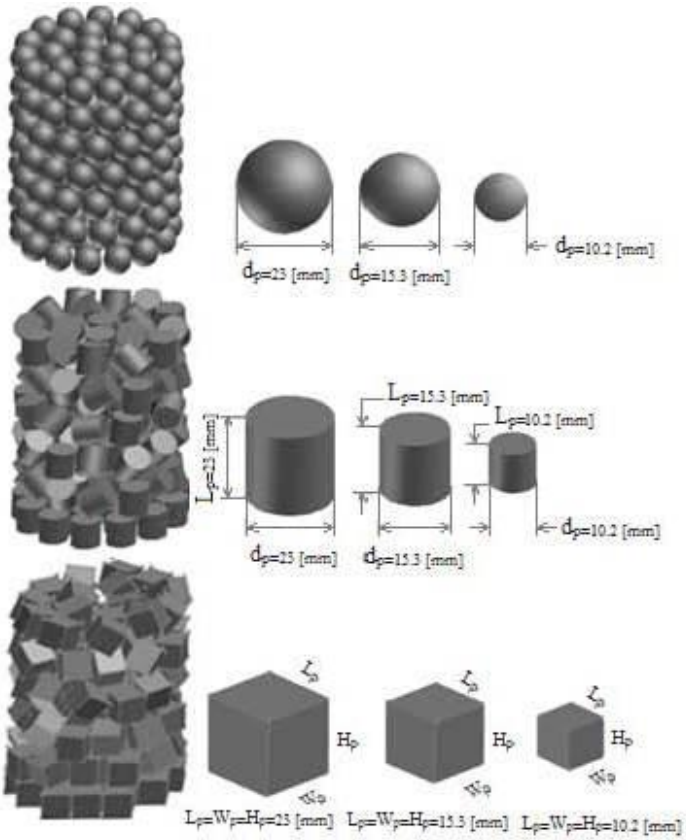

Figure 1

A schematic of the designed beds with spherical, cylindrical, and cubic particles.

The most important step in the simulation is mesh generation. In fact, mesh geometry should be designed in the way that changing the number of meshes does not affect the results, and the geometry must be independent of the mesh. For example, a grid independence study with an unstructured

tetrahedral mesh was carried out in the packed bed with cylindrical particles of N = 6.26 for five different mesh sizes of 5, 4, 3, 2.5, and 2 mm. The pressure drop was evaluated for different mesh sizes, and the optimum one was selected. It was observed that the pressure drop varies to 8.7%, 5.9%, 3.2%, and 0.29% when the grid size is respectively set to 5, 4, 3, 2.5, and 2 mm. As it can be seen from Table 3, at the grid size of 2.5 mm, the pressure drop is independent of mesh size. Therefore, the grid size of 2.5 mm was selected for the simulations of the packed bed with cylindrical particles.

Table 3

Grid independence results for the packed bed with cylindrical particles at N=6.26.

Mesh size (mm)	5	4	3	2.5	2
$\Delta P(Pa)$	0.00854	0.00936	0.00995	0.01028	0.01031
Pressure drop variations		8.7%	5.9%	3.2%	0.29%

4. Results and discussion

4.1. Velocity profiles

The velocity profiles of the packed beds with spherical, cylindrical, and cubic particles and an irregular arrangement at three different bed to particle diameter ratios of N = 4.17, N = 6.26, and N = 9.39 are displayed in Figures 2-4. In these figures, the Reynolds number of the particles is equal to 122.25, 91.69, and 243.81 respectively.

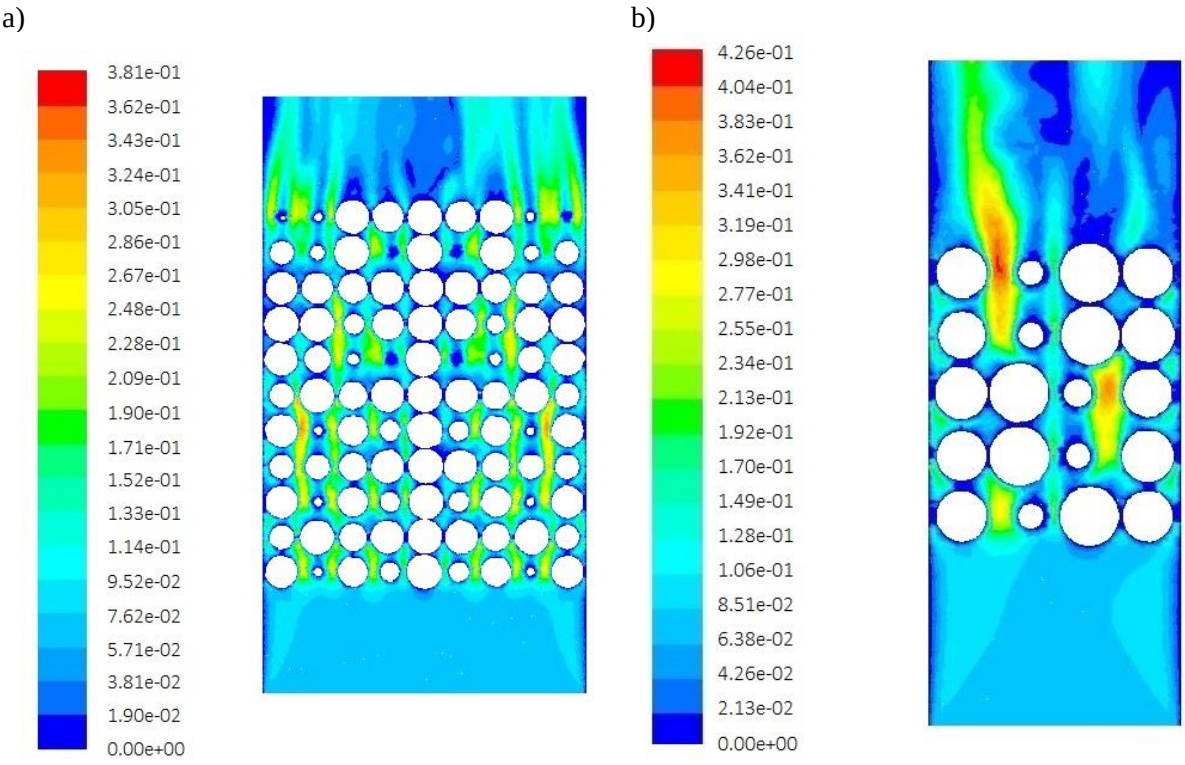

Figure 2

Velocity contour in the packed beds with spherical particles at a Reynolds number of 122.25: a) N = 4.17 and b) N = 9.39.

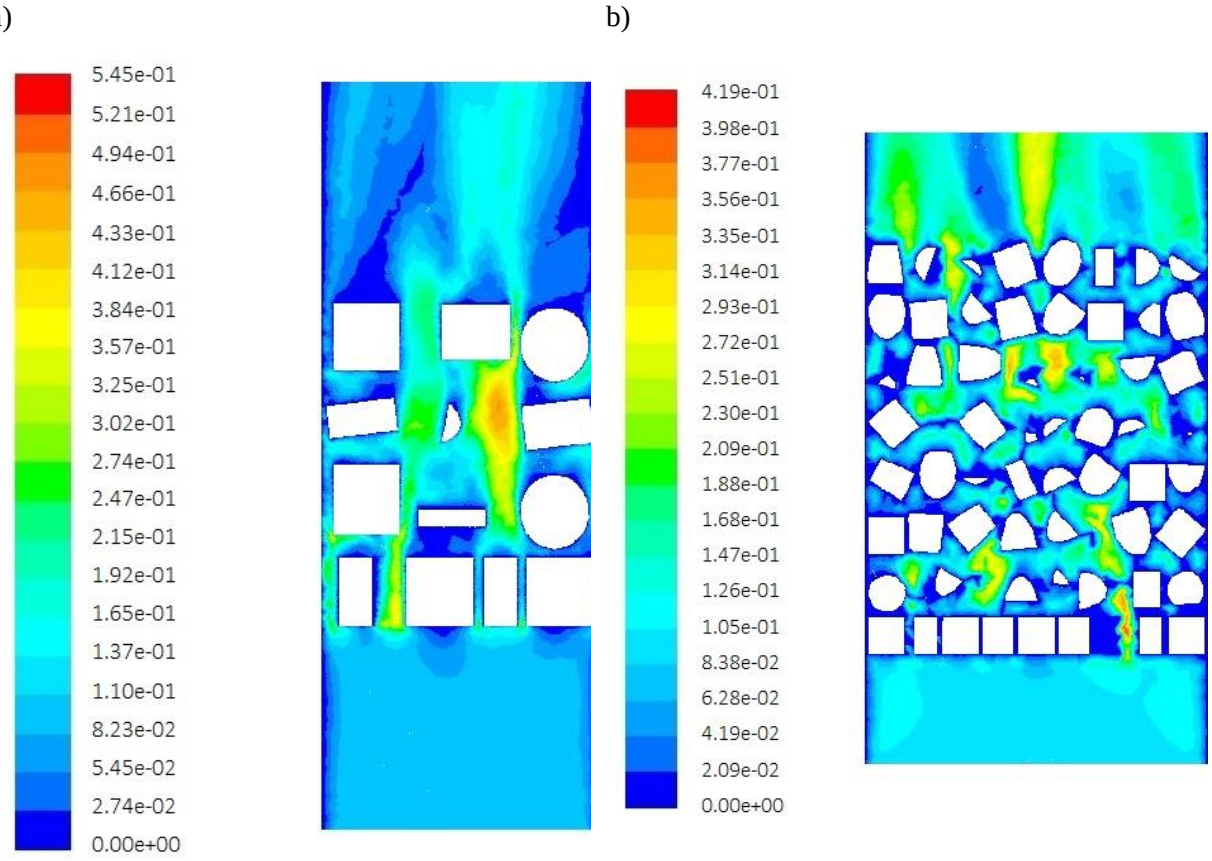

Figure 3

Velocity contour in the packed beds with cylindrical particles at a Reynolds number of 91.69: a) $N = 4.17$ and b) $N = 9.39$.

When the fluid enters the packed bed, it passes through a porous media composed of the particles. In specific regions of the bed where distance between the particle-particle and particle-wall is low, a significant decrease in fluid velocity is observed, and when these distances increase, a uniform velocity profile appears because there is a large crossing surface for fluid flow. As shown in these figures, flow channeling occurs in the parts of the bed having few particles. It can be seen from the contours that flow channeling of the packed bed with cubic particles is more than that of the beds having spherical and cylindrical particles. Flow channeling mostly occurs near the wall, which is due to the cubic shape of particles which cannot cover the region near the wall of the bed. It is also observed that after the collision of the fluid with particles, fluid velocity drops, and it is close to or equal to zero even in this region, which is called the stationary point. The stationary points are more observed in the packed beds with cubic and cylindrical particles because of the flat surface of the particles. However, lower stationary points occur in the packed beds with spherical particles due to their curved shape.

a) b)

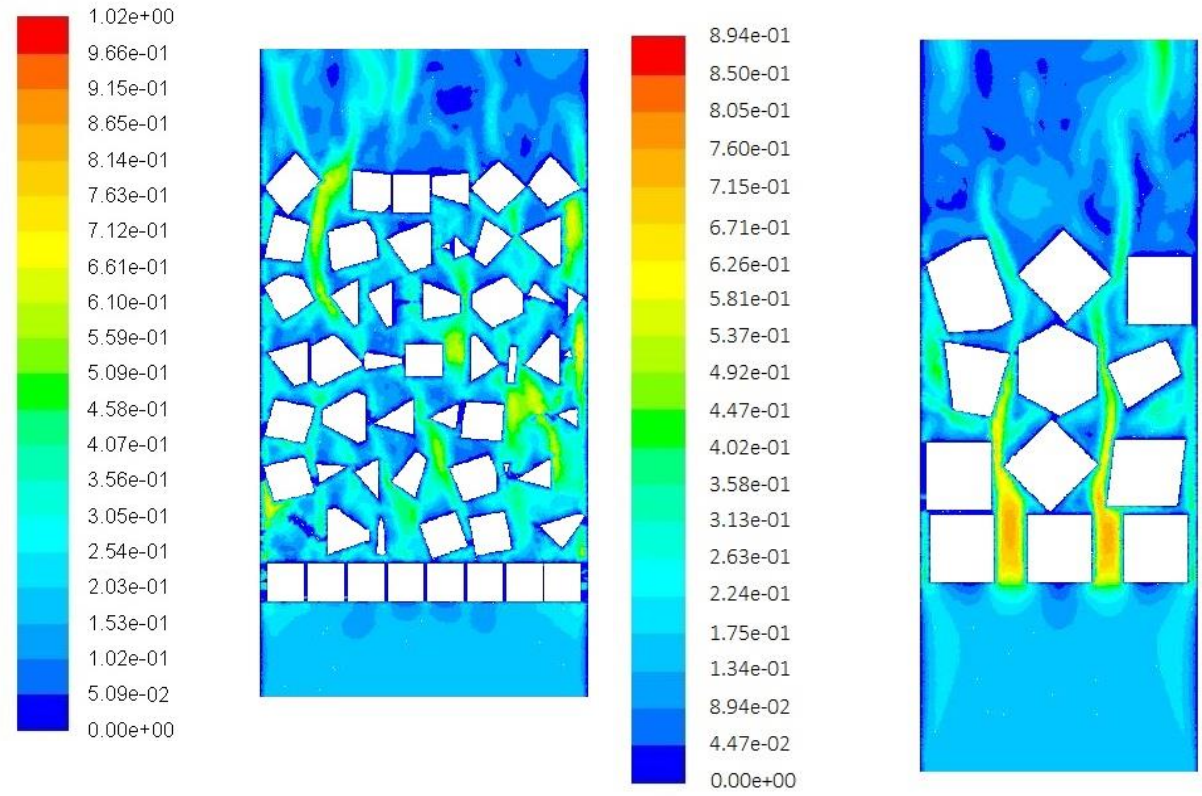

Figure 4

Velocity contour in the packed beds with cubic particles at a Reynolds number of 243.81: a) N = 4.17 and b) N = 9.39.

4.2. Velocity vectors

Velocity vectors in packed beds with spherical, cylindrical, and cubic particles for N = 6.26 at Re_p = 91.69 are illustrated in Figure 5. As it can be observed in this figure, a wake flow is created. This phenomenon is less observed in the packed bed with the spherical particles. The most important parameters making the wake flow in the packed beds can be particle shape, the fluid velocity, and bed void. As shown in Figure 5, wake flow occurs in areas that particles are close to each other. This case is also observed in parts of the bed outlet. With a comparison of the velocity vectors of the three particle types, it can be seen that wake flow in the packed bed with spherical particles is less than that in the packed beds with cylindrical and cubic particles because it is more related to the form of particles; the spherical particles have a curved surface that changes the fluid direction after the fluid collides with particles.

a)

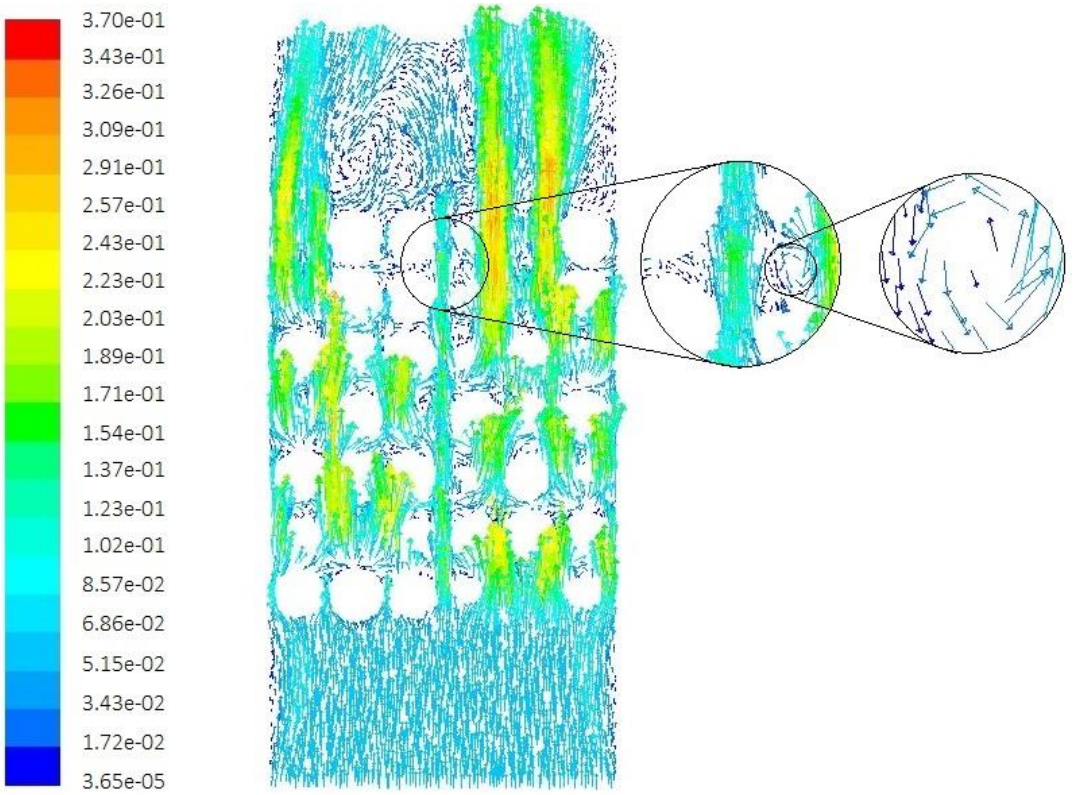
3.70e-01
3.43e-01
3.26e-01
3.09e-01
2.91e-01
2.57e-01
2.43e-01
2.23e-01
2.03e-01
1.89e-01
1.71e-01
1.54e-01
1.37e-01
1.23e-01
1.02e-01
8.57e-02
6.86e-02
5.15e-02
3.43e-02
1.72e-02
3.65e-05

b)

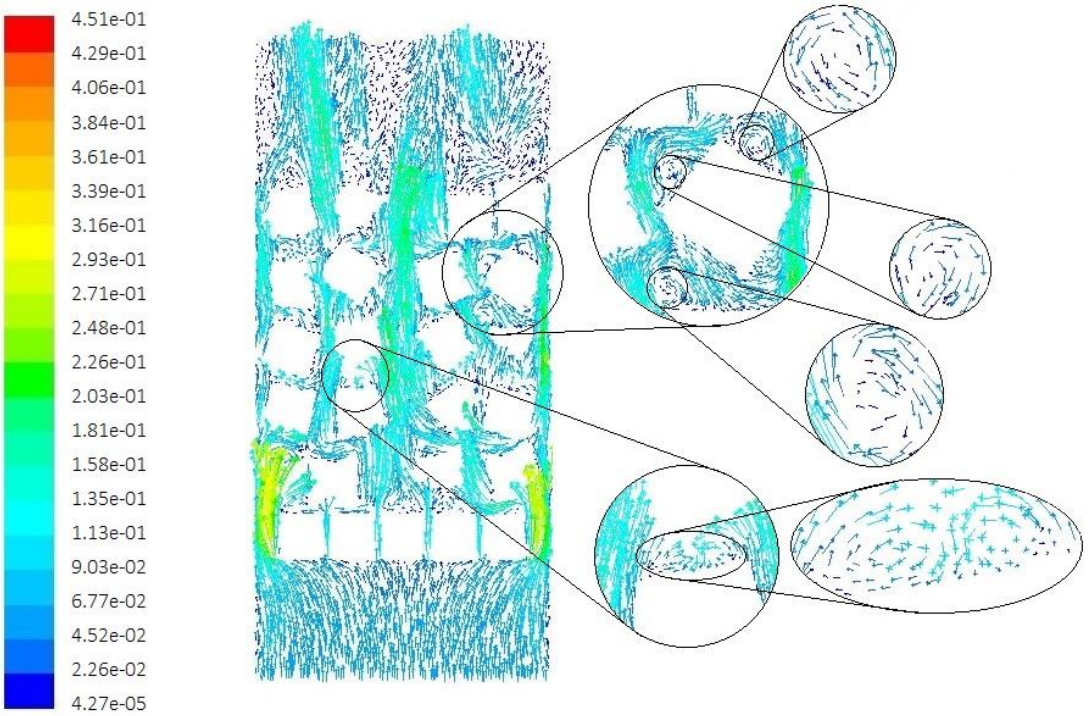
4.51e-01
4.29e-01
4.06e-01
3.84e-01
3.61e-01
3.39e-01
3.16e-01
2.93e-01
2.71e-01
2.48e-01
2.26e-01
2.03e-01
1.81e-01
1.58e-01
1.35e-01
1.13e-01
9.03e-02
6.77e-02
4.52e-02
2.26e-02
4.27e-05

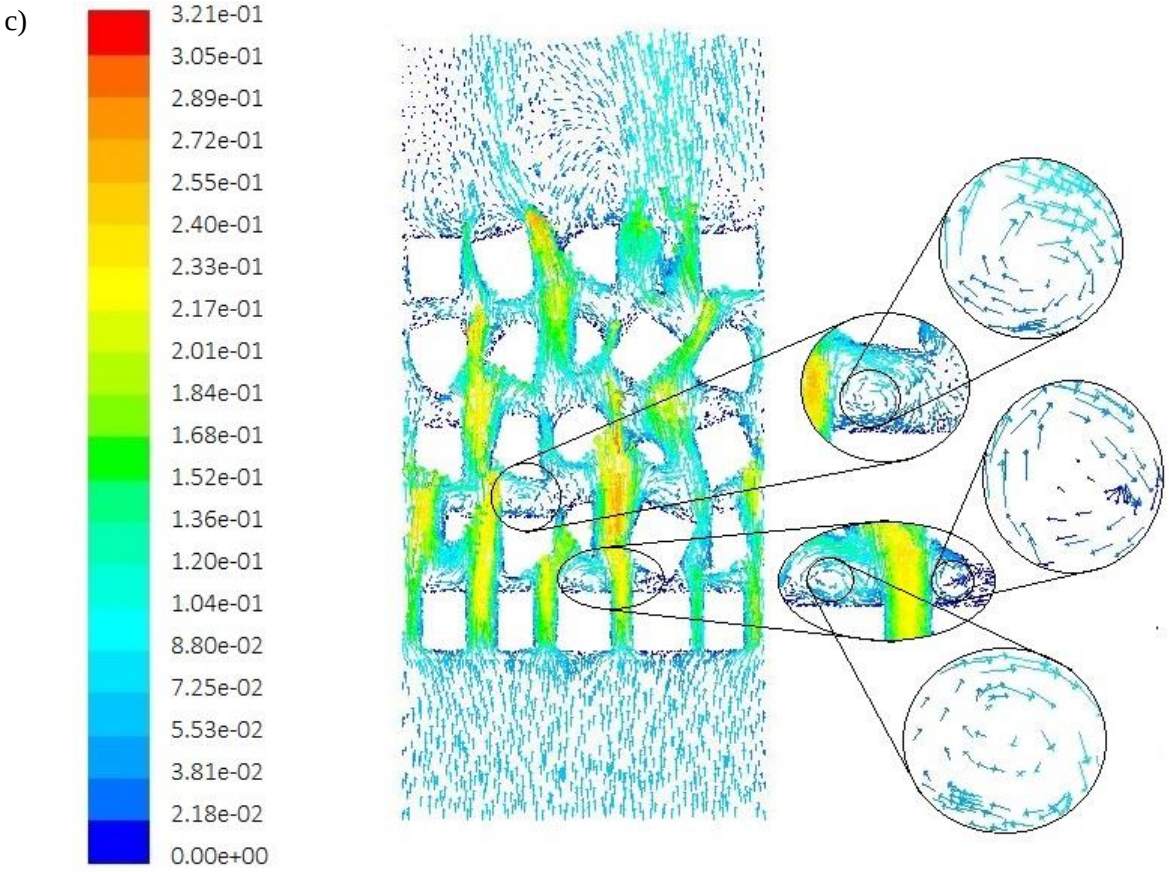

Figure 5

Velocity vectors in the packed beds of N = 6.26 at Rep = 91.69: a) spherical particles, b) cylindrical particles, and c) cubic particles.

4.3. Pressure drop

Since the packed beds are designed for interaction between materials, understanding the hydrodynamics and its related issues such as pressure drop are of great importance in these beds. The fluid pressure drop is the most important parameter in the packed bed design as the heat transfer and mass transfer are strongly relevant to pressure drop. Therefore, the investigation of the parameters influencing pressure drop in packed beds is required. The effect of some parameters such as the length and diameter of bed and the size and shape of particles are studied below.

a. Effect of simultaneous change of the diameter and length of the bed

The pressure drop obtained by CFD simulations for spherical particles at different Reynolds numbers is compared with the empirical equations (Equations 1, 4, and 9) in Figure 6. In order to investigate the effect of the simultaneous change of the diameter and length of the bed, a value of L=1.2D was selected at different ratios of bed to particle diameter. At N = 4.17 and N = 9.39, the bed lengths are 115.2 mm and 259.2 mm respectively. As it can be seen, CFD can well predict the bed pressure drop both quantitatively and qualitatively. It is also found out that the pressure drop of the bed rises by increasing the Reynolds number. The average error of the CFD results in comparison with the empirical equations of Allen et al. (2013), Reichelt (1972), and Ergun (1952) at N = 4.17 is equal to 4.8%, 5.1%, and 6.8% respectively, and it is equal to 5.4%, 3.9%, and 7.8% correspondingly at N = 9.39.

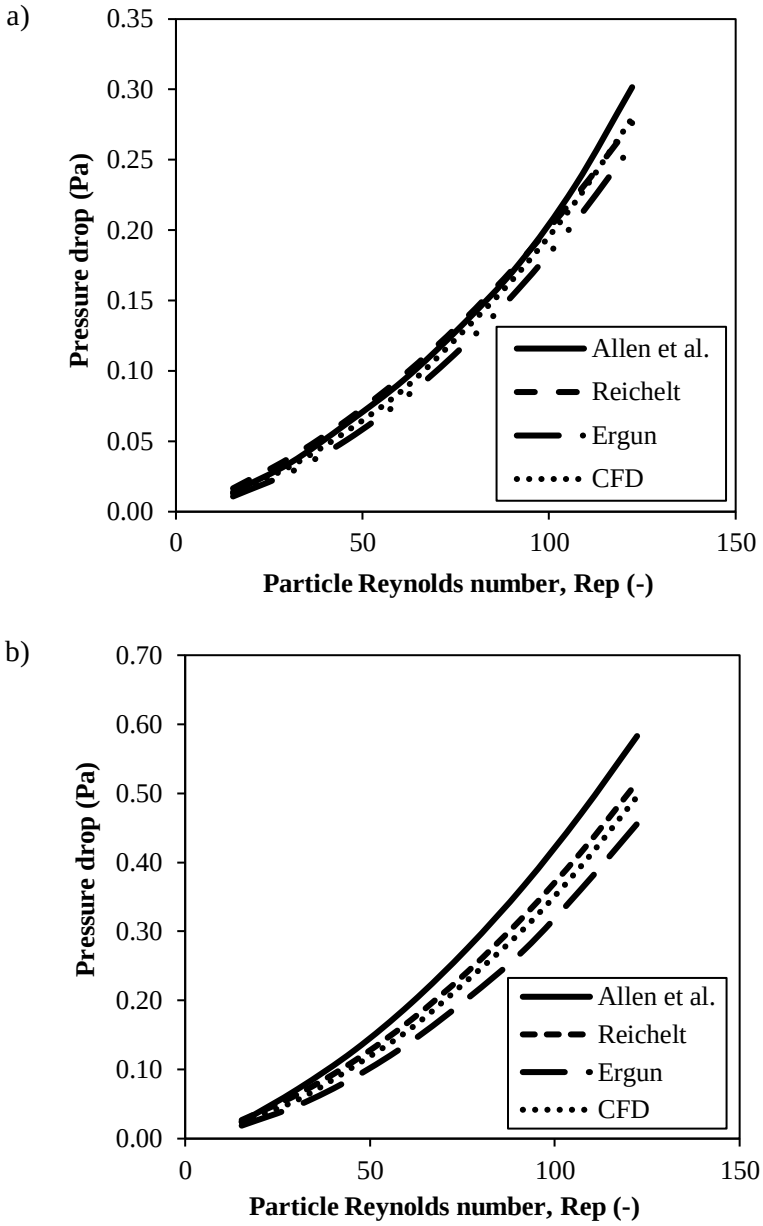

Figure 6

Comparison of the simulated pressure drop with the empirical equations in the packed beds with spherical particles: a) $N = 4.17$ and b) $N = 9.39$.

Figures 7 and 8 show the pressure drop variations versus the particle Reynolds number while simultaneously changing the diameter and length of the packed bed for the cylindrical and cubic particles with N values of 4.17 and 9.39 respectively. According to Figure 7, the average error of the CFD results in comparison with the empirical equations of Allen et al. (2013), Nemec and Levec (2005), Eisfeld and Schnitzlein (2001) is respectively equal to 5%, 3.3%, and 2.8% at $N = 4.17$ and equal to 3.8%, 5.8%, and 2.2% at $N = 9.39$.

It can be seen from Figures 6-8 that the fluid pressure drop increases with raising L and N because higher L and N values cause the fluid to go a longer path along the bed; also, due to the variations of flow pattern and the existence of some forces such as drag force, the pressure drop enhances. For example, by comparing the pressure drop for the three packed beds with spherical, cylindrical, and

cubic particles, it is observed that at N = 4.17 and Re_p = 122.25 the pressure drop of the fluid in the beds with spherical, cylindrical, and cubic particles is equal to 0.2797 Pa, 0.2069 Pa, and 0.191 Pa respectively, while it is equal to 0.4952 Pa, 0.3689 Pa, and 0.3998 Pa at N = 9.39 respectively. The main reason for this difference is the bed porosity because the porosity of the beds for spherical particles with N = 4.17 and N = 9.39 is about 55% and 54% respectively, while beds with cylindrical particles have a porosity of about 60.7% and 57.6% at N = 4.17 and N = 9.39 respectively; the porosity of beds with cubic particles is about 62.5% and 58.6% at N = 4.17 and N = 9.39 respectively.

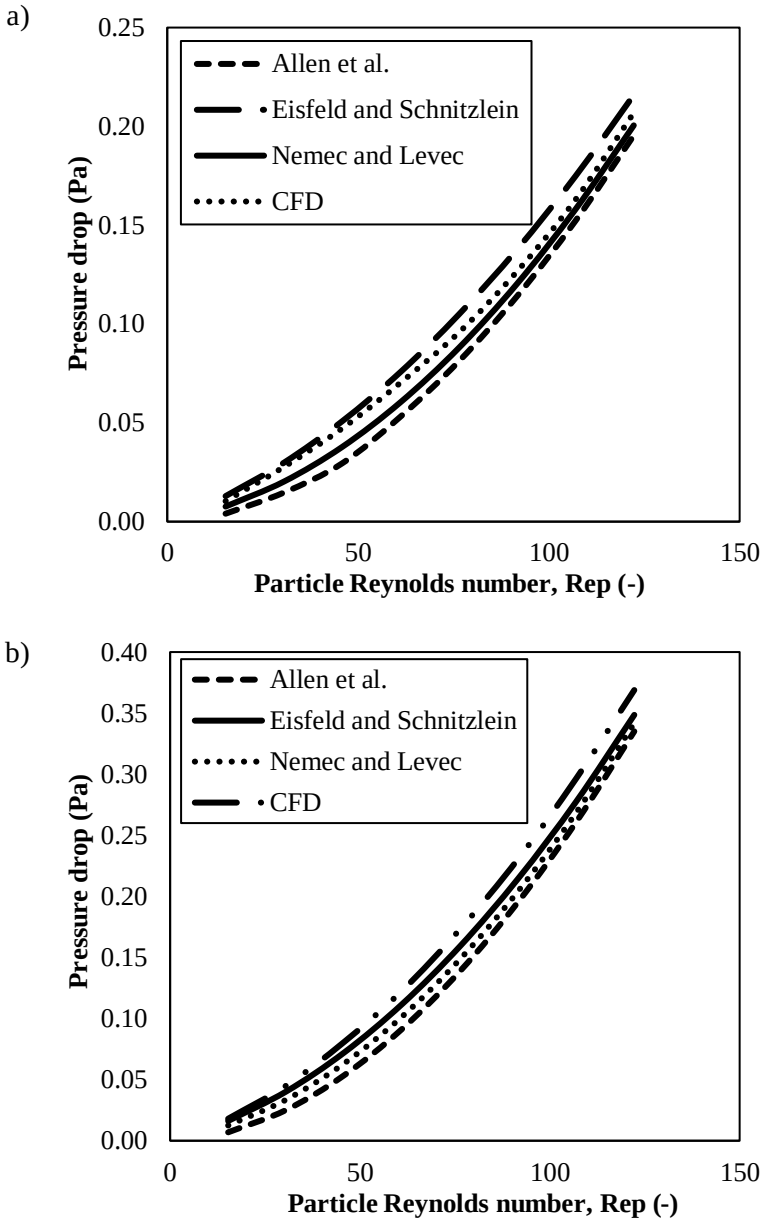

Figure 7

Comparison of the simulated pressure drop with empirical equations in the packed beds with cylindrical particles: a) N = 4.17 and b) N = 9.39.

b. Effect of bed length

The pressure drop variations of the fluid through the bed at different lengths of the bed are illustrated in Figure 9. The simulations were conducted for two ratios of N = 6.26 and N = 9.39 at three different bed lengths of $L = 0.8D$, $L = D$, and $L = 1.2D$. Figure 9 depicts the trend of pressure drop variations for the packed bed with spherical particles (a, b), cylindrical particles (c, d), and cubic particles (e, f). As it can be seen, the longer bed lengths cause higher fluid pressure drops because the fluid passes a longer path along the packed bed in comparison with the beds that have a lower length.

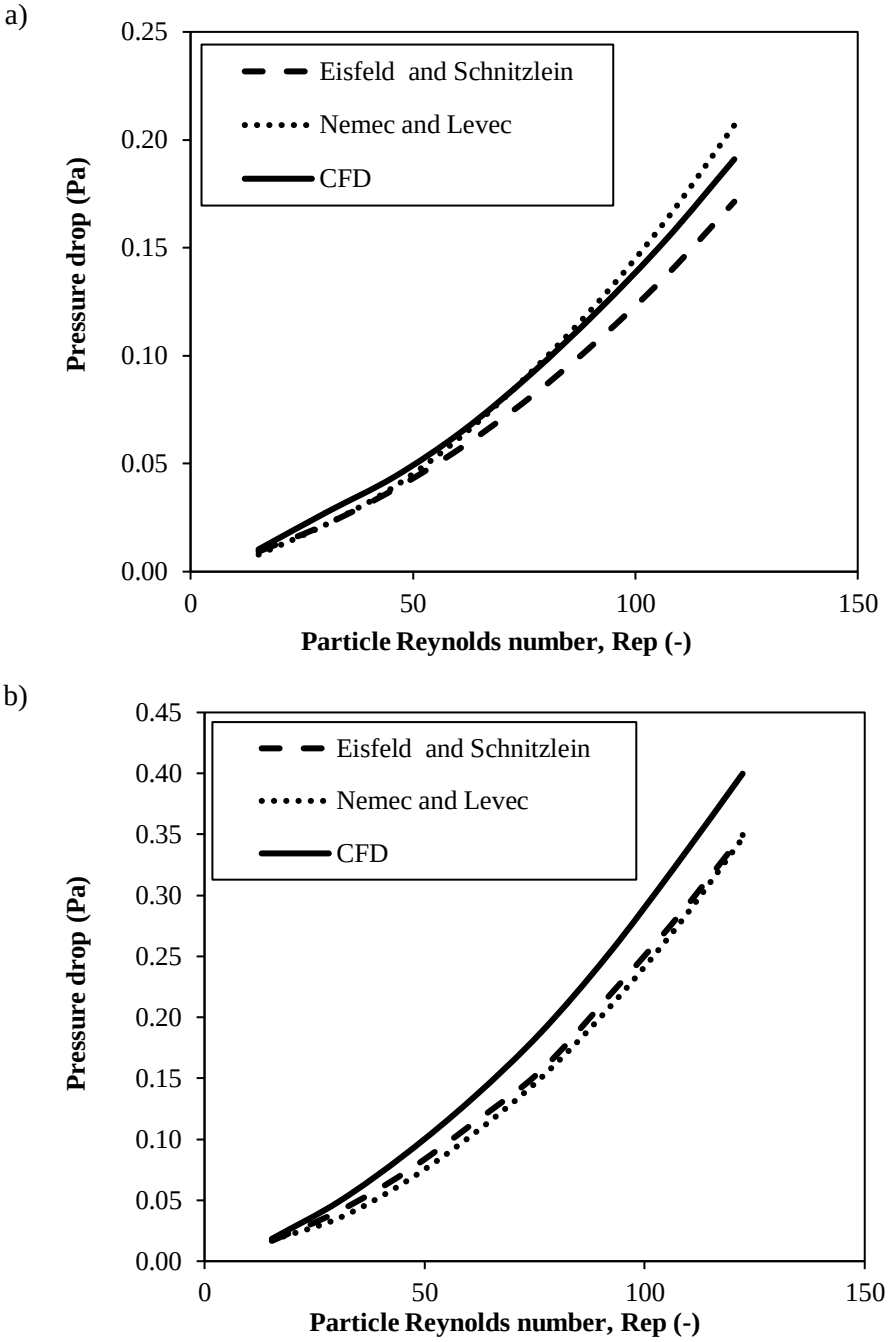

Figure 8

Comparison of the simulated pressure drop with empirical equations in the packed beds with cubic particles: a) N = 4.17 and b) N = 9.39.

a)

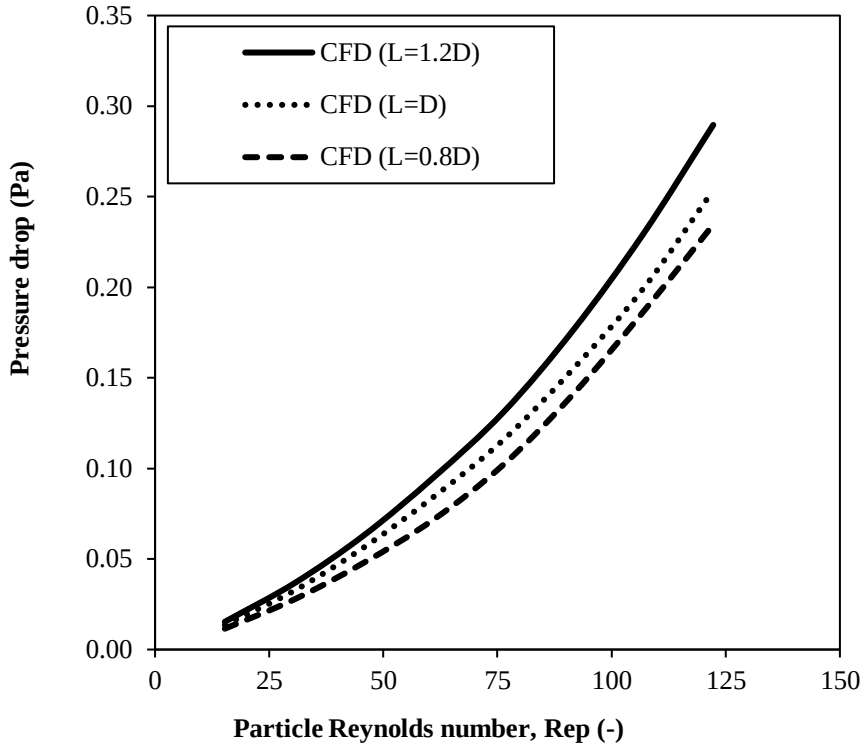
CFD (L=1.2D)
CFD (L=D)
CFD (L=0.8D)
Pressure drop (Pa)
0.35
0.30
0.25
0.20
0.15
0.10
0.05
0.00
0
25
50
75
100
125
150
Particle Reynolds number, Rep (-)

b)

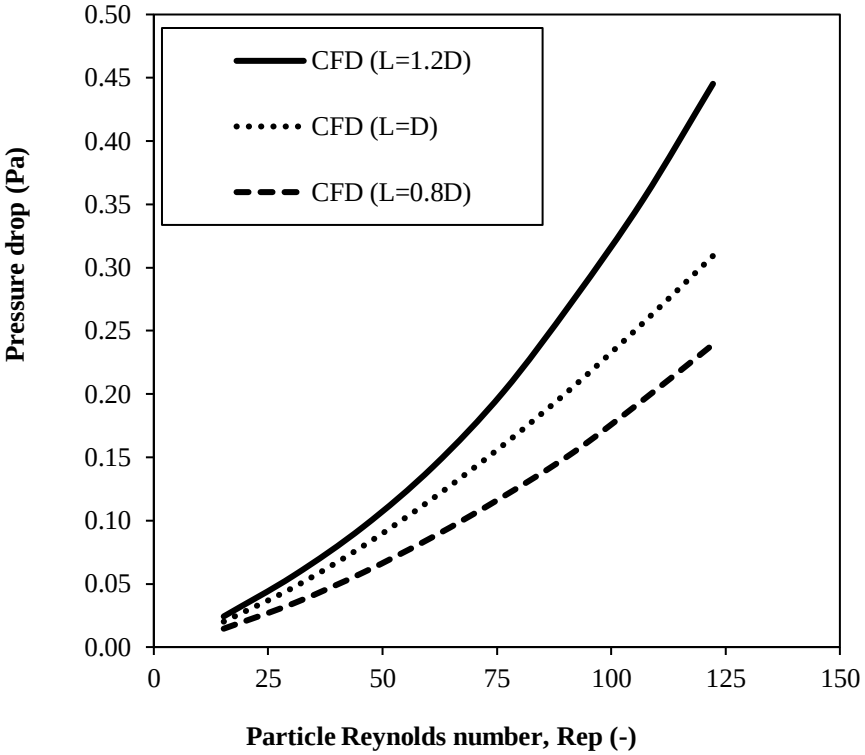
CFD (L=1.2D)
CFD (L=D)
CFD (L=0.8D)
Pressure drop (Pa)
0.50
0.45
0.40
0.35
0.30
0.25
0.20
0.15
0.10
0.05
0.00
0
25
50
75
100
125
150
Particle Reynolds number, Rep (-)

c)

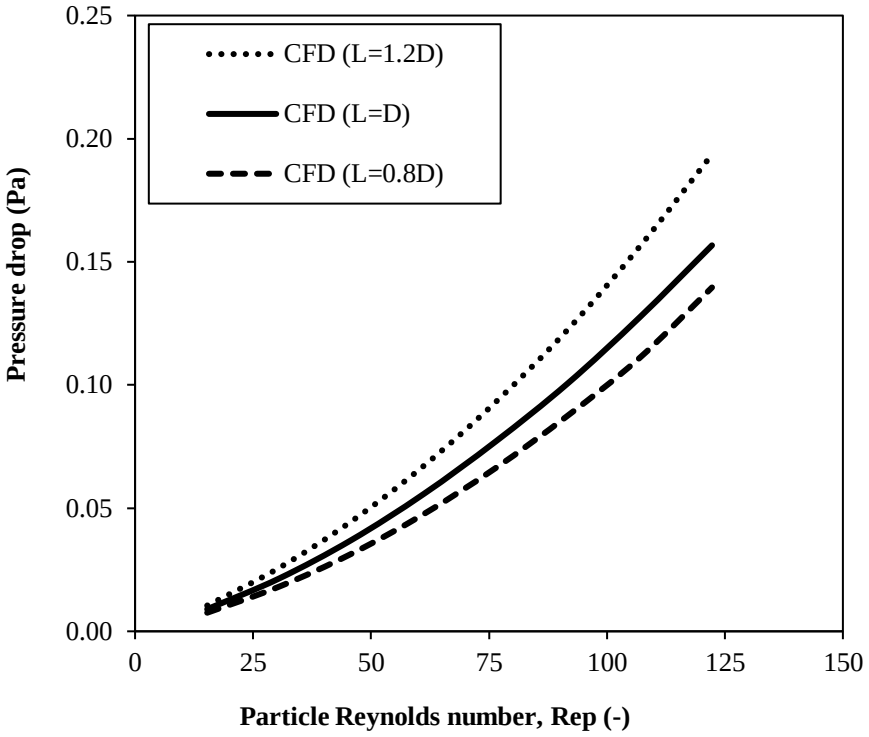
CFD (L=1.2D)
CFD (L=D)
CFD (L=0.8D)
Pressure drop (Pa)
0.25
0.20
0.15
0.10
0.05
0.00
0
25
50
75
100
125
150
Particle Reynolds number, Rep (-)

d)

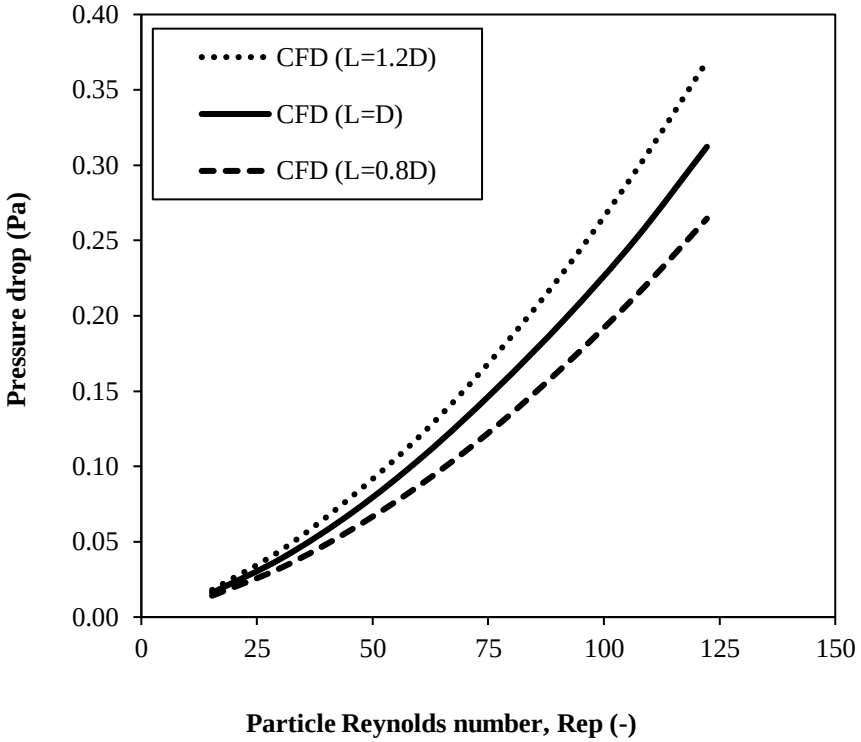
CFD (L=1.2D)
CFD (L=D)
CFD (L=0.8D)
Pressure drop (Pa)
0.40
0.35
0.30
0.25
0.20
0.15
0.10
0.05
0.00
0
25
50
75
100
125
150
Particle Reynolds number, Rep (-)

e)

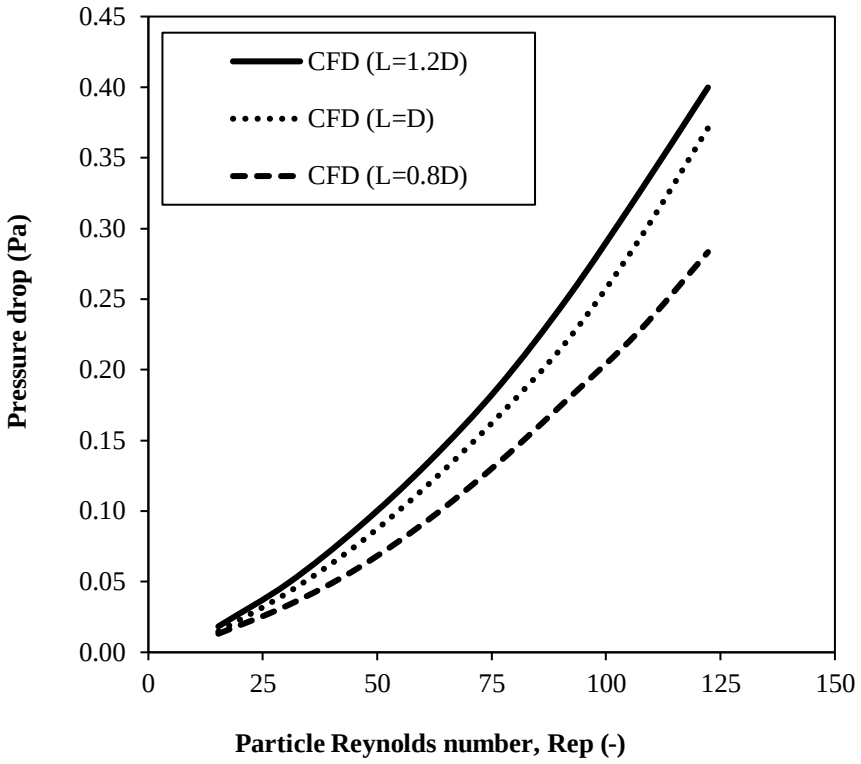

f)

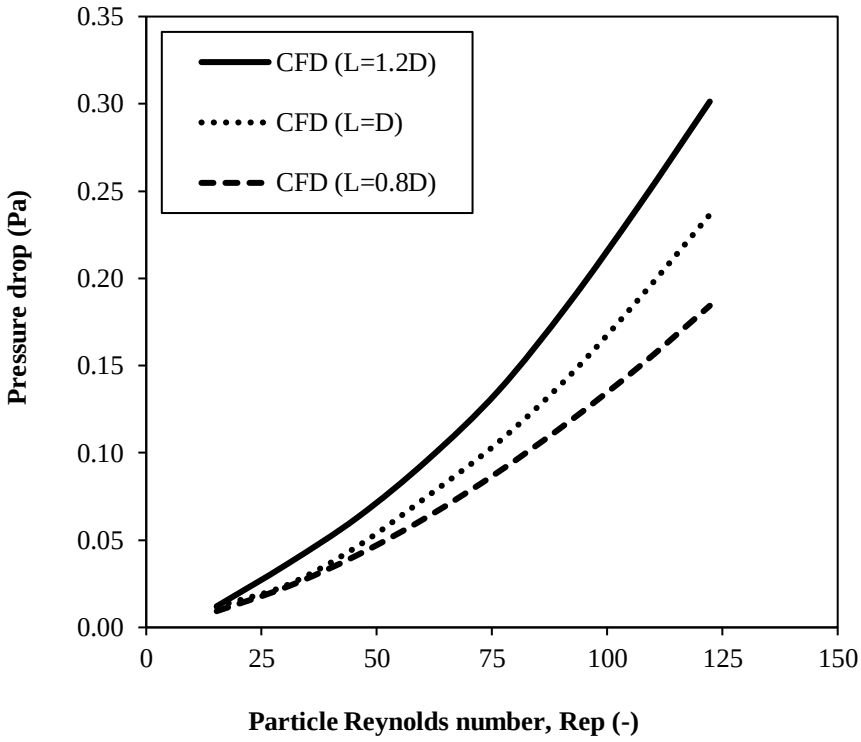

Figure 9

Variations of the simulated pressure drop versus the particle Reynolds number: a) spherical particles with N = 6.26; b) spherical particles with N = 9.39; c) cylindrical particles with N = 6.26; d) cylindrical particles with N = 9.39; e) cubic particles with N = 6.26, and f) cubic particles with N = 9.39.

c. Effect of particle size

The effect of particle size on pressure drop at a constant diameter of the bed is displayed in Figure 10, where the simulation results at three different ratios of bed to particle diameter of N = 4.17, N = 6.26, and N = 9.39 and at a bed length of 115.2 mm and a bed diameter of 96 mm are illustrated. It should be noted that, in the simulations, the spherical particles were considered at three different diameters of 23 mm (N = 4.17), 15.33 mm (N = 6.26), and 10.22 mm (N = 9.39). The cylindrical particles were also selected at three different sizes of $L_p = d_p$ = 23 mm, $L_p = d_p$ = 15.33 mm, $L_p = d_p$ = 10.22 mm; the parameters related to the cubic particles are as follows too: $L_p = W_p = H_p$ = 23 mm, $L_p = W_p = H_p$ = 15.33 mm, and $L_p = W_p = H_p$ = 10.22 mm.

a)

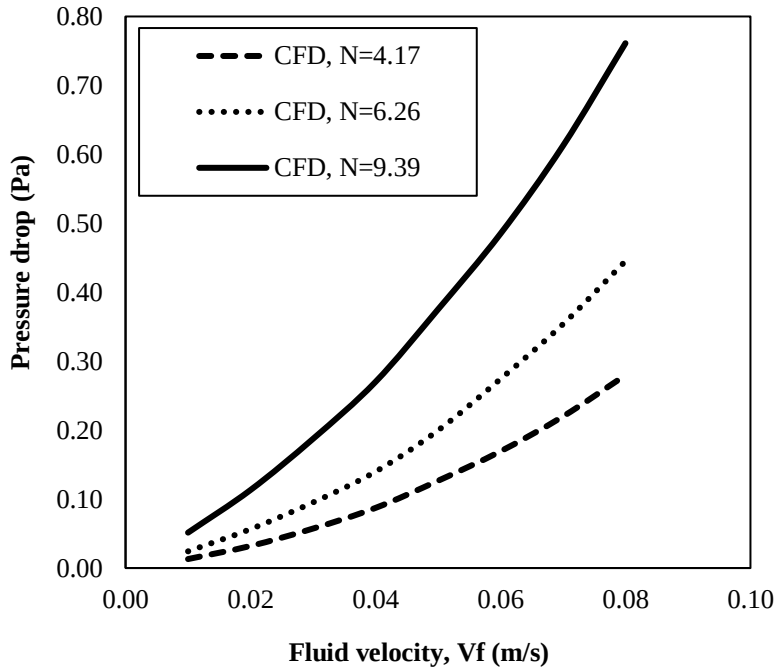

b)

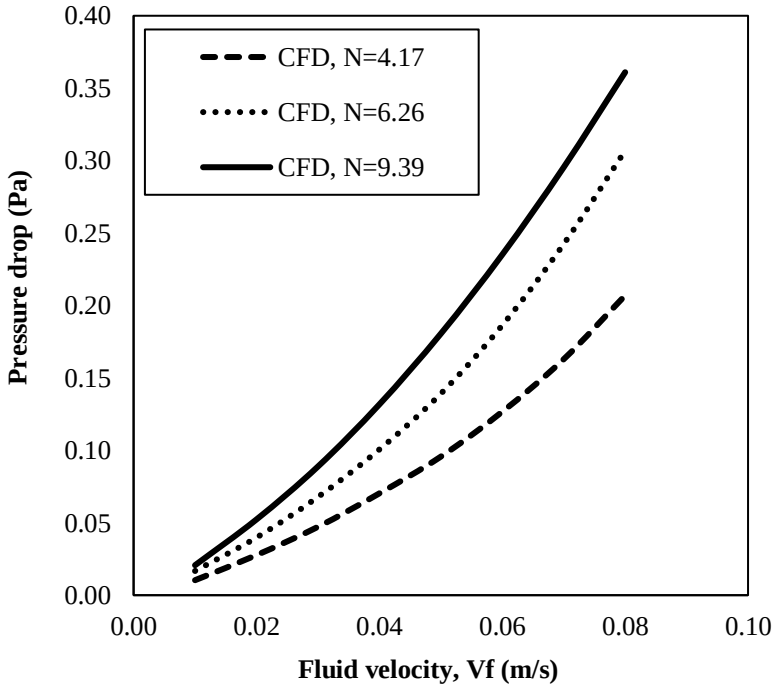

c)

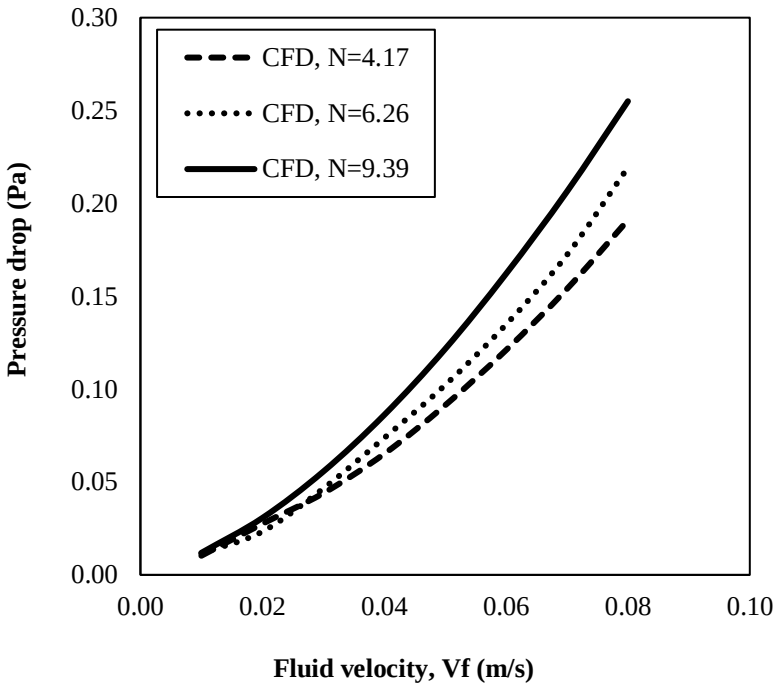

Figure 10

Effect of particle size on pressure drop versus fluid velocity: a) spherical particles, b) cylindrical particles, and c) cubic particles.

By comparing Figures (10-a), (10-b), and (10-c), it can be seen that the pressure drop rises at a higher bed to particle diameter ratio. For example, the pressure drop for packed bed with spherical particles at V_f = 0.08 m/s is equal to 0.2792 Pa, 0.4452 Pa, and 0.7612 Pa at respectively N = 4.17, N = 6.26, and N = 9.39. It is equal to 0.2069 Pa, 0.3069 Pa, and 0.361 Pa for cylindrical particles and equal to 0.191 Pa, 0.225 Pa, and 0.3249 Pa for cubic particles. This pressure difference between the different shapes of particles is due to bed porosity created by particles. For example, in the packed bed with spherical particles at N = 9.39, the bed porosity is about 55%, while the packed beds with cylindrical and cubic particles at the same ratio (N) have a porosity of about 63.6% and 61.5% respectively. Thus, when the porosity of the bed enhances, the fluid pressure drop decreases because the fluid has more space to pass through the particles. If the porosity of the beds becomes equal, other factors such as wake flow and the existence of drag force, which is different due to the shape of particles, can affect the fluid pressure drop with different particles.

4.4. Packed beds with different particle types

A packed bed containing a combination of three particle types of spherical, cylindrical, and cubic was designed using three different ratios of bed to particle diameter of N = 4.17, N = 6.26, and N = 9.39 while the diameter and length of the bed are simultaneously changed. The sizes of the spherical, cylindrical, and cubic particles are respectively equal to d_p = 23 mm, $L_p = d_p$ = 23 mm, and $L_p = W_p = H_p$ = 23 mm. The CFD simulation results of this packed bed are as follows:

a. Velocity profiles

Figures 11 and 12 respectively depicts the velocity contours and vectors for N = 4.17 and N = 9.39 at a Reynolds number of particles equal to 106.97. It can be seen that channeling occurs in the parts of the bed which are not covered by particles and or have few particles. After the collision of the fluid

with the particles in the bed, stagnation points are created. According to these figures, further stagnation points are observed around the cubic and cylindrical particles because of their flat surfaces, and fewer stagnation points occur around the spherical particles due to their curved shape.

a)

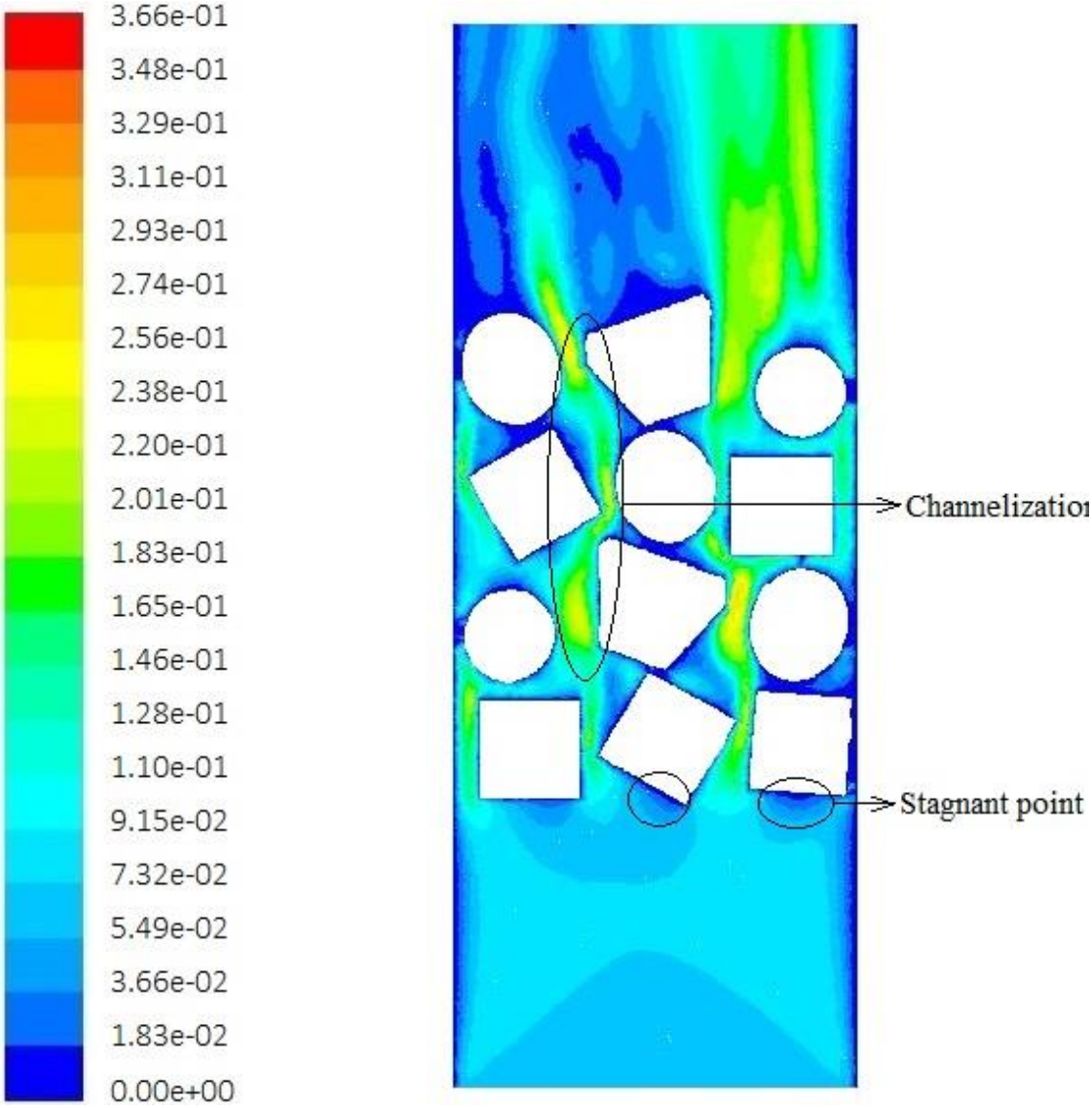

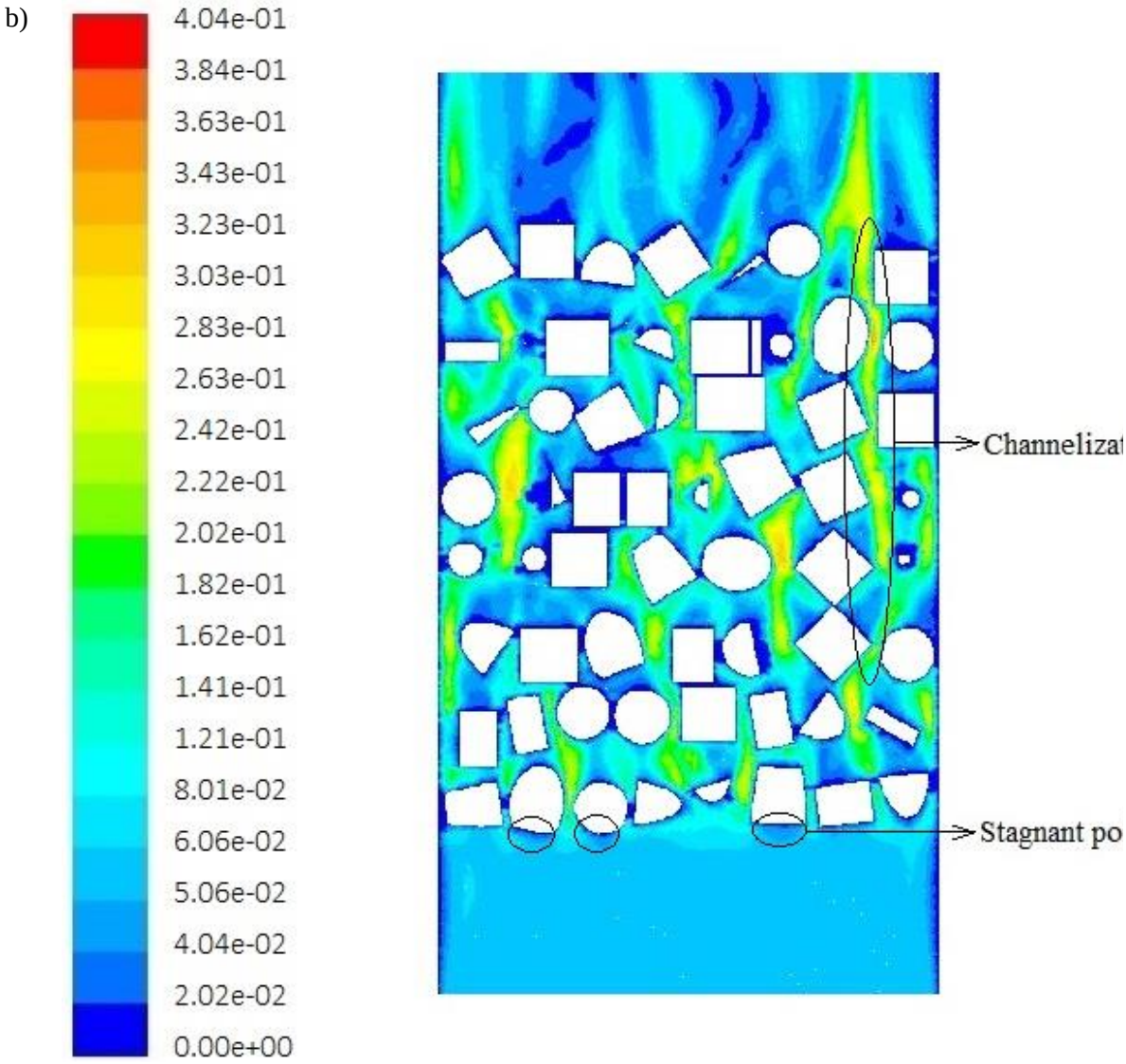

Figure 11

Velocity counters in the packed bed containing different particle types at *Rep* = 106.97: a) *N* = 4.17 and b) *N* = 9.39.

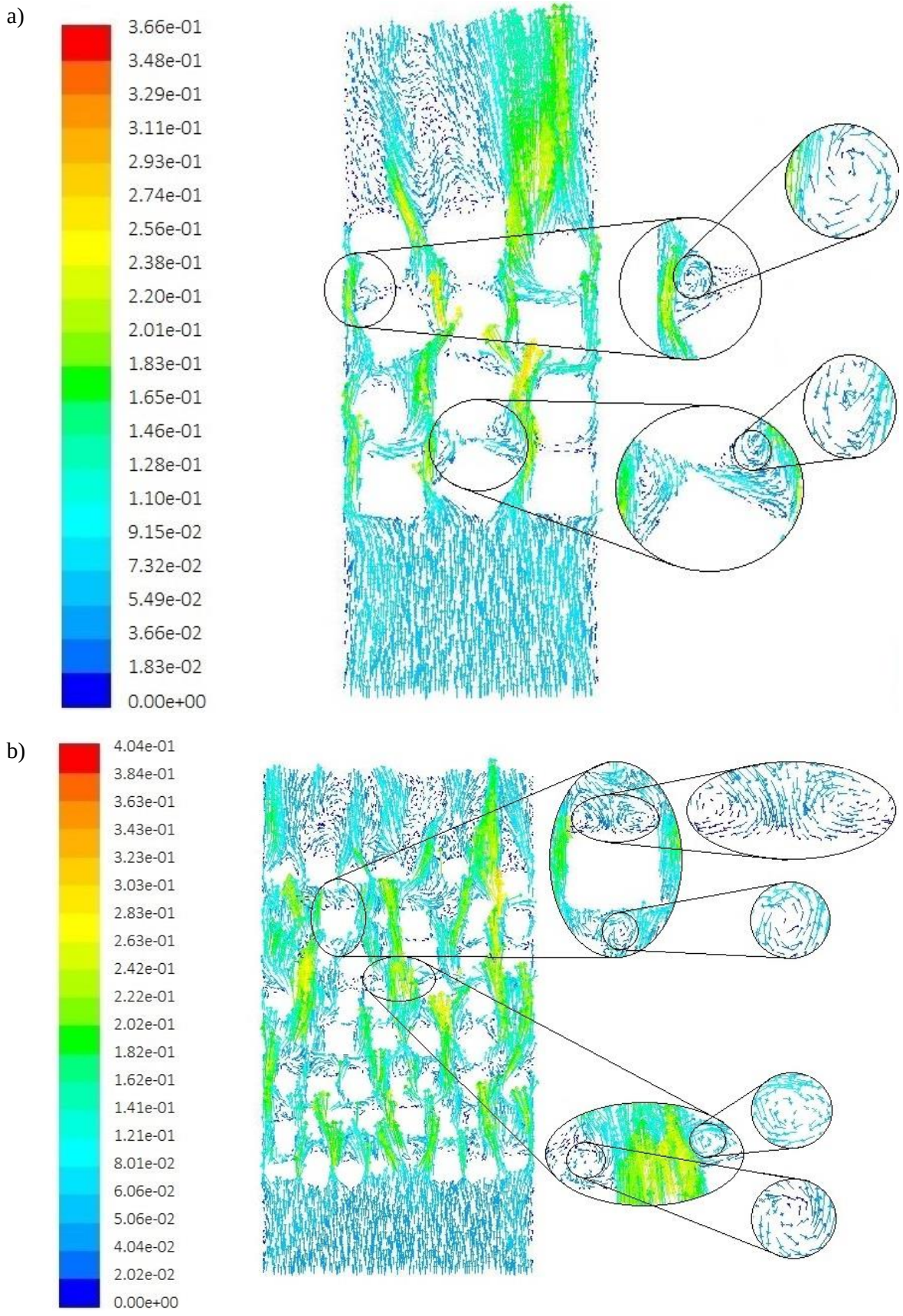

Figure 12

Velocity vectors in the packed bed containing different particle types at *Rep* = 106.97: a) *N* = 4.17 b) *N* = 9.39.

b. Pressure drop

The comparison of the pressure drop obtained by the CFD simulations in the packed beds having a combination of different particles at three different ratios of bed to particle diameter of N = 4.17, N = 6.26, and N = 9.39 with the empirical equation of Eisfeld and Schnitzlein (2001) is illustrated in Figure 13. It is obvious that the simulated pressure drop values are overestimated due to wake flow and viscose forces effects in the bed. The average errors of the CFD results in comparison with the empirical equation of Eisfeld and Schnitzlein (2001) at N = 4.17, N = 6.26, and N = 9.39 are respectively equal to 3.2%, 8.9%, and 7.9%.

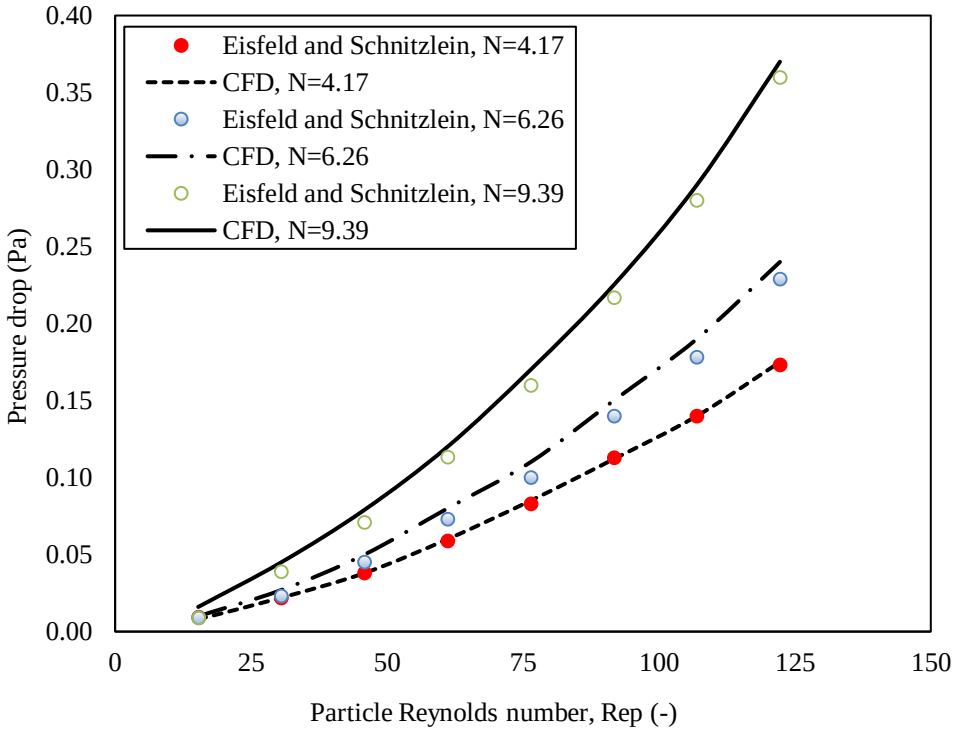

Figure 13

Pressure drop versus particle Reynolds number in the packed bed having different particle types for N = 4.17, N = 6.26, and N = 9.39.

5. Conclusions

In the current work, the characteristics of fluid flow and pressure drop along beds with a low ratio of bed to particle diameter for spherical, cylindrical, and cubic particles were investigated. The numerical simulations were also carried out for a combination of three particle types in the bed. The empirical equations were utilized in order to validate the CFD simulation results.

The contours of fluid flow within all the beds showed that fluid velocity increases in specific regions where the distance between the particle-particle and particle-wall is long. It was also seen that flow channeling occurs in the parts of bed which are not suitably covered by particles. According to the CFD simulations, uniform velocity profiles appear when distances are increased because there is a more crossing surface for fluid flow. The velocity vectors indicated that some phenomena such as wake and vortex flows are created in the beds packed with flat surface particles.

It was also found out that the pressure drop varies for each particle type at different lengths and diameters of the bed. As the simulation results stated, the pressure drop of the bed rises by a

simultaneous increase in the diameter and length of the bed. The effect of particle size on the pressure drop for three packing types confirmed that the pressure drop increases by reducing the particle size because at a higher number of particles in the bed the fluid cannot easily flow.

By comparing the pressure drop of the beds containing different particle shapes, it was confirmed that the fluid pressure drop is greater in the beds packed with spherical particles than those packed with cylindrical and cubic particles. The main reason for this difference is the bed porosity created by particles. For beds containing different particle types but having equal porosity, the pressure drop depends on wake flow and the existence of forces such as drag force, which differ according to the shape of particles. Moreover, the pressure drop of the bed packed with a combination of three particle types is lower than that of the beds packed with similar particles. Finally, we suggest that the simulations should be performed to calculate the heat and mass transfer coefficients in the bed packed with a combination of particles.

Nomenclature

A_p	Particle surface area, (m^2)
A_w	Wall correction term, (-)
B_w	Wall correction term, (-)
D	Bed diameter, (m)
d_h	Hydraulic diameter, (m)
d_p	Particle diameter, (m)
d_{sv}	Equivalent surface volume diameter, (m), $d_{sv} = \frac{6 \,.\, V_p}{\varphi \,.\, A_p}$
K	Constant in Equations 4 and 7, (-)
k_1, k_2	Constants in Equation 5, (-)
L	Length of packed bed, (m)
L_p	Length of cylindrical particle, (m)
M	Wall correction term, (-)
N	Bed to particle diameter ratio, $N = \frac{D}{d_p}$
n_p	Particle number in the bed
Re_{duct}	Duct Reynolds number, (-), $Re_{duct} = \frac{2 \,.\, \rho \,.\, u_s \,.d_p}{3 \,.\, \mu\,(1-\varepsilon)}$
Re_p	Particle Reynolds number, (-), $Re_p = \frac{\rho \,.\, u_s \,.d_p}{\mu}$
u_s	Superficial velocity, (m/s)
V_p	Particle volume, (m^3)
V_b	Bed volume, (m^3)
Greek symbols	
ΔP	Pressure drop, (Pa)
ε	Porosity, (-), $\varepsilon = 1 - \frac{n_p \, V_p}{V_p}$

μ_f	Fluid dynamic viscosity, $\left(\frac{kg}{m.s}\right)$
ρ_f	Fluid density, $\left(\frac{kg}{m^3}\right)$
Φ	Particle sphericity, (-)

References

Allen, K. G., von Backstrom, T. W., and Kroger, D. G., Packed Bed Pressure Drop Dependence on Particle Shape, Size Distribution, Packing Arrangement and Roughness, Powder Technology, Vol. 246, p. 590-600, 2013.

Ancheyta, J., Munoz, J. A. D., and Maceas, M. J., Experimental and Theoretical Determination of the Particle Size of Hydrotreating Catalysts of Different Shapes, Catalysis Today, Vol. 109, p. 120-127, 2005.

Andrigo, P., Bagatin, R., and Pagani, G., Fixed Bed Reactors, Catalysis Today, Vol. 52, p. 197-221, 1999.

ANSYS FLUENT 12.0.16: Theory Guide, ANSYS, Inc., 2009.

Atmakidis, T. and Kenig, E. Y., CFD-based Analysis of the Wall Effect on the Pressure Drop in Packed Beds with Moderate Tube/Particle Diameter Ratios in the Laminar Flow Regime, Chemical Engineering Journal, Vol. 155, p. 404-410, 2009.

Bayati, B., Ejtemaei, M., Charchi Aghdam, N., Babaluo, A. K., Mohammad Haghighi, M., and Sharafi, A., Hydro-isomerization of n-Pentane over Pt/Mordenite Catalyst: Effect of Feed Composition and Process Conditions, Iranian Journal of Oil & Gas Science and Technology, Vol. 5, p. 84-99, 2016.

Calis, H. P. A., Nijenhuis, J., Paikert, B.C., Dautzenberg, F. M, and van den Bleek, C. M., CFD Modelling and Experimental Validation of Pressure Drop and Flow Profile in a Novel Structured Catalytic Reactor Packing, Chemical Engineering Science, Vol. 56, p. 1713-1720, 2001.

Du, W., Quan, N., Lu, P., Xu, J., Wei, W., and Zhang, L., Experimental and Statistical Analysis of the Void Size Distribution and Pressure Drop Validations in Packed Beds, Chemical Engineering Research and Design, Vol. 106, p. 115-125, 2016.

Eisfeld, B. and Schnitzlein, K., The Influence of Confining Walls on the Pressure Drop in Packed Beds, Chemical Engineering Science, Vol. 56, p. 4321-4329, 2001.

Ergun, S., Fluid Flow through Packed Columns, Chemical Engineering Progress, Vol. 48, p. 89-94, 1952.

Foumeny, E. A., Benyahia, F., Castor, J. A. A., Moallemi, H. A., and Roshani, S., Correlations of Pressure Drop in Packed Beds Taking into Account the Effect of Confining Wall, International Journal of Heat and Mass Transfer, Vol. 36, p. 536-540, 1993.

Ghaemi, A., Hashemzadeh, V., and Shahhosseini, Sh., An Experimental Investigation of Reactive Absorption of Carbon Dioxide into an Aqueous $NH_3/H_2O/NaOH$ Solution, Iranian Journal of Oil & Gas Science and Technology, Vol. 6, p. 55-67, 2017.

Golshadi, M., Mosayebi Behbahani, R., and Irani, M., CFD Simulation of Dimethyl Ether Synthesis from Methanol in an Adiabatic Fixed-bed Reactor, Iranian Journal of Oil & Gas Science and Technology, Vol. 2, p. 50-64, 2013.

Guo, Z., Sun, Zh., Zhang, N., Ding, M., and Wen, J., Experimental Characterization of Pressure Drop in Slender Packed Bed ($1 < D/d < 3$), Chemical Engineering Science, Vol. 173, p. 578-587, 2017.

Mehta, D. and Hawley, M. C., Wall Effect in Packed Columns, Industrial and Engineering Chemistry Design and Development, Vol. 8, p. 280-282, 1969.

Moazami, N., Wyszynski, M. L., Mahmoudi, H., Tsolakis, A., Zou, Z., Panahifar, P., and Rahbar, K., Modelling of a Fixed Bed Reactor for Fischer-Tropsch Synthesis of Simulated N_2-Rich Syngas over Co/SiO_2: Hydrocarbon Production, Fuel, Vol. 154, p. 140-151, 2015.

Montillet, A., Akkari, E., and Comiti, J., About a Correlating Equation for Predicting Pressure Drop through Packed Beds of Spheres in a Large of Reynolds Numbers, Chemical Engineering Processing: Process Intensification, Vol. 46, p. 329-333, 2007.

Nemec, D. and Levec, J., Flow through Packed Bed Reactors: 1. Single-phase Flow, Chemical Engineering Science, Vol. 60, p. 6947-6957, 2005.

Rase, H. F., Fix-bed Reactor Design and Diagnostics: Gas-phase Reactions, 1st Ed., Elsevier, 1990.

Reddy, R. K. and Joshi, J. B., CFD Modeling of Pressure Drop and Drag Coefficient in Fixed Beds: Wall Effects, Particuology, Vol. 8, p. 37-43, 2010.

Reichelt, W., Berechnung Des Druckverlustes Einphasig Durchstr Mter Kugel-und Zylinderschüttungen, Chemie Ingenieur Technik, Vol. 44, p. 1068-1071, 1972.

Vollmari, K., Oschmann, T., Wirtz, S., and Kruggel-Emden, H., Pressure Drop Investigations in Packings of Arbitrary Shaped Particles, Powder Technology, Vol. 271, p. 109-124, 2015.

Zhao, J., Li, S., Lu, P., Meng, L., Li, T., and Zhu, H., Shape Influences on the Packing Density of Frustums, Powder Technology, Vol. 214, p. 500-505, 2011.